Chromosome Research **11**: 537–547, 2003.

Four-dimensional imaging of chromatin dynamics during the assembly of the interphase nucleus

E. M. M. Manders[1†], A. E. Visser[1,3†], A. Koppen[1], W. C. de Leeuw[2], R. van Liere[2], G. J. Brakenhoff[1] & R. van Driel[1*]
[1]*Swammerdam Institute for Life Sciences, BioCentrum Amsterdam, University of Amsterdam, Kruislaan 318, 1098 SM Amsterdam, The Netherlands; Tel: +31.20.525.5150; Fax: +31.20.525.7924; E-mail: van.driel@science.uva.nl;* [2]*Center for Mathematics and Computer Science, CWI, Amsterdam, The Netherlands;* [3]*Current address: The Scripps Research Institue, Department of Cell Biology, La Jolla, USA*
**Correspondence*
[†]*Authors Manders and Visser have contributed equally to this work*

Key words: cell cycle, chromatin, confocal microscopy, four-dimensional imaging, interphase nucleus, nuclear organization

Abstract

Large-scale chromatin organization is likely to play an important role in epigenetic control of gene expression. This implies that after mitosis the correct chromatin organization must be re-established in the nuclei of the two daughter cells. Here we analyze the dynamic behavior of chromatin during the transition from late anaphase to G1 in dividing HeLa cells, which express green fluorescent protein-tagged histone H2B. Time-lapse confocal microscopy was used to image the movement and the decondensation of chromatin as cell division progresses. Typically, time series of over 100 three-dimensional images (4D images) were collected, spanning a time period of up to three hours. Special care was taken to avoid photodamage, since cell cycle progression is exquisitely sensitive to photochemical damage. Quantitative analysis of the 4D images revealed that during the anaphase to G1 transition the movement of chromatin domains relative to other chromatin is remarkably limited. Chromatin dynamics can best be described as a radial expansion of the cluster of chromosomes that is present in late anaphase. We find that decondensation occurs in two phases. First a rapid decondensation by about a factor of two, followed by a slower phase in which part of the chromatin does not decondense any further, whereas the remaining chromatin decondenses further about two fold.

Introduction

Chromatin of eukaryotic cells is not homogeneously distributed throughout the interphase nucleus. First of all, each individual chromosome occupies a discrete domain in the nucleus, called chromosome territory (Hens *et al.* 1983, Cremer *et al.* 1993). Within a territory, multiple compact chromatin domains can be discerned, surrounded by interchromatin space that is largely devoid of DNA (Cmarko *et al.* 1999, Verschure *et al.* 1999). A close relationship exists between large-scale chromatin folding and transcriptional activity. For instance, positioning of a locus near a

pericentromeric heterochromatin domain results in its silencing (Fisher & Merkenschlager 2002). Evidently, large-scale chromatin organization in the nucleus is an important element in epigenetic gene control.

As large-scale chromatin organization is important, special molecular mechanisms must exist that ensure the correct relative positioning and condensation state of chromosomal domains in the newly formed G1 nucleus. Despite its importance, it is still obscure how large-scale chromatin organization is established in the cell nucleus. In this study, we address this fundamental problem by analyzing chromatin dynamics as cells proceed from late anaphase into G1-interphase. To do so, we have examined living HeLa cells that stably express GFP-tagged histone H2B (Kanda *et al.* 1998) by four-dimensional (4D) imaging, i.e. time lapse three-dimensional (3D) confocal scanning microscopy.

A major problem in live cell imaging is the phototoxicity of the light used for excitation of the fluorophore, in this case GFP. We have addressed this problem by carefully optimizing each step in the imaging process, thereby minimizing the harmful exposure of cells to the laser light during 4D imaging. Results show that chromatin moves radially away from the initial compact lump of chromosomes present in late anaphase. We observe remarkably little relative movement of different chromosomes. The implications of these observations are discussed.

Materials and methods

Cell culture

A HeLa cell line stably expressing histone H2B-GFP (cell line 2–12-HeLa; Kanda *et al.* 1998) was kindly provided by Dr H. Kimura (University of Oxford, Oxford, UK). Cells were grown in DMEM (Gibco, Life Technologies Ltd, Paisley, UK) supplemented with 10% FCS (Gibco), glutamine and penicillin/streptavidin at 37°C and 5% CO_2 in glass-bottom microdishes (MatTek, Ashland, MA). Two hours before imaging, the medium was replaced by prewarmed DMEM without phenol red (Gibco) supplemented with 10% FCS, glutamine, penicillin/streptavidin and free radical scavenger Trolox (0.1 mmol/L; Sigma-Aldrich Chemie BV, Zwijndrecht, The Netherlands). The glass-bottom plate was placed on a heated microscope stage (37°C, Zeiss, Jena, Germany). An objective heater (Bioptech, Butler, PA) was used to keep the microscope objective at 37°C. To stabilize the temperature, cell cultures (60% confluent) were kept on the microscope stage for at least 2 h prior to imaging.

Live cell 4D microscopy

Images were captured with a Zeiss LSM510 using a Plan-Neofluar $100\times/1.3$-oil objective (Zeiss, Jena, Germany). For live cell imaging, the laser power of an Ar-ion laser (15 mW; 488 nm) was set at 25% of its maximum power and the AOTF was tuned down to 1% to minimize light exposure of the cells. This resulted in a laser power of less than 150 nW measured at the point of imaging. On the basis of differential interference contrast (DIC) cells that had entered mitosis were selected. Subsequently, sequences of between 100 and 150 3D images were acquired during a period of 2–3 h. The sampling frequency varied between one and fifteen 3D images per 5 min, depending on the rate of chromatin movement. The number of optical sections per 3D image varied between 12 and 30 sections per image, depending on the thickness of the cell. The step size along the z-axis was 0.7 μm. Each x–y optical section had a size of 256×256 pixels, each pixel being 120×120 nm. The integration time for each pixel was 1.7 μs. No Kalman filtering (averaging over several sections) was used in order to minimize light exposure time. Typically, the integrated light dose during the acquisition of a 4D image (time series of 3D images) under these conditions was 10 Jcm^{-2}. The detection pinhole was tuned at 2.0 Airy units, matching the axial sampling rate to obtain 3D images with an acceptable signal-to-noise ratio. We have recorded eleven 4D images of dividing cells and selected three of them for extensive analysis. Simultaneously with the time sequence of 3D confocal images, a series of DIC images were collected to inspect cell morphology during and after 4D imaging.

Analysis of time sequences of 3D images

Time series of 3D images of living cells were analyzed using the image analysis and processing software ScilImage (TNO, Delft, The Netherlands; Van Balen *et al.* 1994), supplemented with dedicated routines, running on a Silicon Graphics workstation (SGI, Mountain View, CA). 4D images were first corrected for cellular and nuclear movement by aligning the center of the nucleus (center of mass) of all 3D images in the time sequence and a rotation correction procedure, based on the alignment of local maxima of intensity (Manders *et al.* 1996), was performed. Chromatin movement was analyzed with dedicated software 'BM3D' (De Leeuw & Van Liere 2002). The algorithm is based on a block-matching technique, which fits two subsequent 3D images from a time sequence, by a series of local elastic transformations. This procedure allows tracking of any point in a 4D image. Local maxima and local minima of intensity in the last 3D image of the time series were determined and back-tracked in time. The intensity of these minima and maxima were measured at all time-points. Tracks of local minima and local maxima were plotted (Figure 2). We have developed dedicated virtual reality techniques for visual inspection of 4D images and tracks (De Leeuw *et al.* 2000, De Leeuw & Van Liere 2001). This method allowed us to obtain detailed insight into chromatin movement in the living cell.

Results

Experimental conditions that minimize photochemical damage and photobleaching

Phototoxic effects due to excitation light often limit the analysis of living cells by 3D and 4D (3D plus time) fluorescent microscopy. We have optimized our imaging system so that high-quality 3D images can be obtained by scanning confocal microscopy at a high rate over a period of several hours. In experiments where we exposed cells to a high dose of light, phototoxicity induced complete cell cycle arrest (data not shown), most likely due to DNA damage (Manders *et al.* 1999). Cell cycle progression evidently is a sensitive measure for photodamage. Therefore, we only used imaging conditions that did not slow down progression through the cell cycle as non-damaging.

In our experiments, we have minimized phototoxicity as follows: (1) reducing the excitation light intensity as much as possible, (2) minimizing the total exposure time of the cell, and (3) adding a free radical scavenger (Trolox) to the culture medium. To reduce exposure time, we adapted throughout the experiment the sampling frequency and the number of optical sections per 3D image to the actual rate of chromatin movement and to the thickness of the cell. Consequently, the sampling rate decreased from three 3D images per min during late anaphase, to one image per 5 min as the cell entered G1 interphase. In addition, as cells are still rounded up in anaphase, 3D images were made up of 30 optical sections, whereas later on, as the daughter cells flatten upon entering G1, 12 sections per 3D image were sufficient. The total exposure time of the cell during a typical time series of 3D images was only 70 s over a period of 2.5 h. The combination of the low excitation light intensity (150 nW) and short total exposure time (70 s) resulted in a total light dose of only 10 μJ over 2.5 h. Under these conditions progression through mitosis was not retarded and therefore the cells were most likely undamaged.

In all experiments we started recording the time sequences of 3D images in late anaphase. One of the two daughter cells was 4D imaged for about 2.5 h, from late anaphase into G1, and consequently was exposed to excitation light. The other daughter cell remained in the dark and was used as a control. At the end of the time series, it was impossible to distinguish the exposed cell from its unexposed sister cell based on cell morphology (data not shown). These observations indicate that the exposed cell is not affected by the exposure to light. Therefore, we conclude that there is no detectable phototoxic effect of the excitation light under our experimental conditions.

Chromatin decondensation at the end of mitosis involves minimal chromatin movement

During the transition from late anaphase to G1-interphase, chromatin is highly dynamic. In addition the nucleus is moving as a whole. Therefore, the 4D images were corrected for

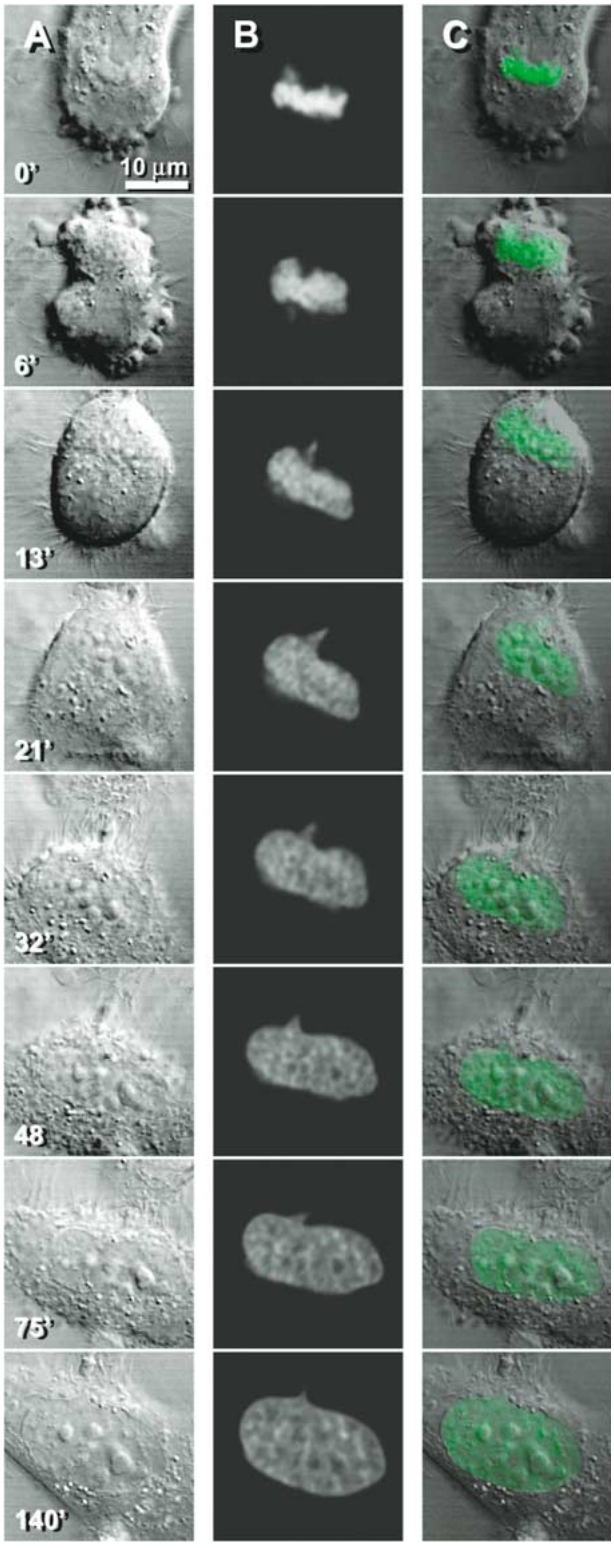
A
B
C
0'
10 µm
6'
13'
21'
32'
48
75'
140'

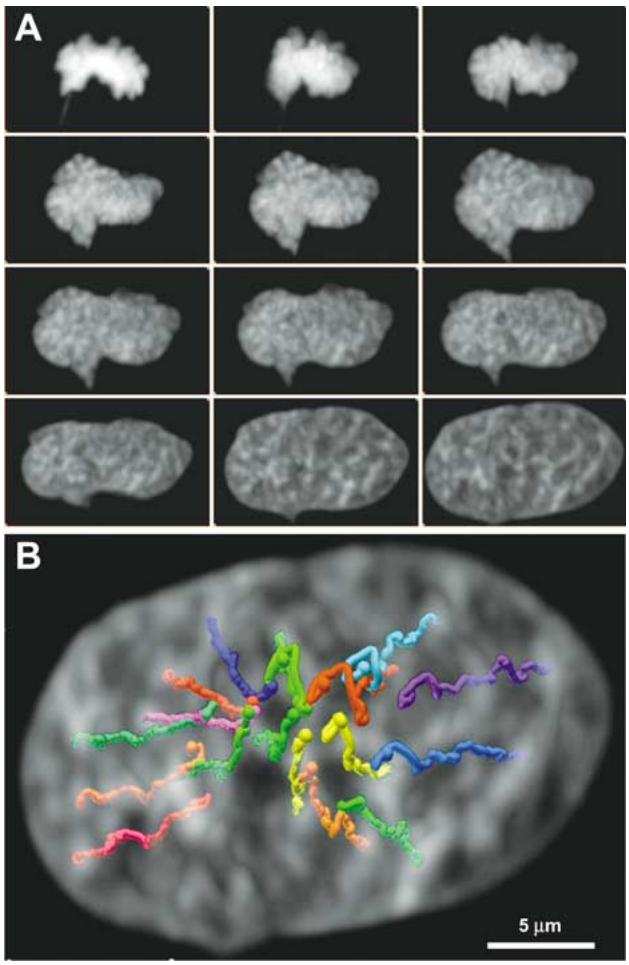

Figure 2. Directional chromatin movement during late anaphase–G1 transition. Individual compact chromatin domains can be discriminated early after anaphase. Most of these domains remain relatively condensed throughout the anaphase–G1 transition. **(A)** shows these compact chromatin domains at 9 time points (the images represent the sum of all the optical sections of a 3D image). Several such domains have been followed in time and space from late anaphase well into G1. The colored lines in **(B)** are tracks in time and space, representing the movement of individual chromatin domains, superimposed on the gray-value image representing the sum of all the optical sections in the last 3D image (140 min). Results show that compact chromatin domains migrate radially away from the center of the nucleus as chromatin decondensation and nuclear assembly proceeds.

Figure 1. Chromatin dynamics during the late anaphase–G1 transition. **(A)** Differential interference contrast images of a time series of a dividing HeLa cell, starting at $t = 0$ min in late anaphase and ending at $t = 140$ min well in G1. **(B)** Same cell and time sequence as shown in **(A)**. Histone H2B-GFP signal in eight midnuclear optical sections of a time series of 135 3D images (12–30 optical sections each). The first image was captured immediately after anaphase. **(C)** Shows the merged image of **(A)** and **(B)**. Only one daughter cell is imaged. The other daughter cell is kept in the dark. At the end of anaphase (0 min), as the chromosomes have been pulled towards the spindle poles, individual chromosomes can no longer be discerned. After a few minutes, chromatin starts to differentiate into compact and less-compact domains (6–13 min). As the cell proceeds into G1, more structures in terms of compact and less-compact domains, as well as nucleoli, are observed.

translation and rotation of the nucleus (see Methods section). The processed 4D images show the dynamics of chromatin during the anaphase to G1 transition process, including movement and decondensation. Figure 1 shows a typical time series chosen from eleven of such 4D images made with these cells. The left column (A) of Figure 1 shows the DIC image and the time (in minutes) after imaging started in late anaphase. The central column (B) shows a single mid-nuclear optical section from the 3D image stack, and the right column (C) displays an overlay of the DIC image and the fluorescence image. We have focused on a number of condensed chromatin domains and followed their fate throughout anaphase to G1 transition. Although the nature of these domains is not known, some of them may represent centromeric structures. Trajectories representing the movement of condensed chromatin domains in time and space were determined using dedicated tracking software. The trajectories are displayed in Figure 2. Each color represents the dynamic behavior (trajectory) of an individual condensed chromatin domain. The 3D tracks in Figure 2D are projected on a gray-value image representing the sum of all optical sections of the cell. Interestingly, essentially all compact chromatin domains move outwards in a radial manner as chromatin decondenses and the new G1 nucleus is formed. Further visual inspection of the time series of 3D images shows that, throughout the process, the movement of compact chromatin domains relative to each other is remarkably limited. Evidently, chromatin domains that are adjacent in late anaphase remain neighbors in G1. All of the analyzed 4D images show this behavior.

All chromatin is decondensed after mitosis

Figure 1 shows a selection of eight time points from a 4D image data set consisting of 135 3D images, covering a period of 2.5 h from late anaphase into interphase G1. Within a few minutes after imaging starts, the tight lump of chromosomes begins to open up and domains with low local chromatin concentration begin to appear. The nuclear envelope can be discerned by differential interference contrast after about 20–30 min (Figure 1A: images at 21 and 32 min). During the same period, the cell flattens and attaches to the glass surface of the incubation chamber. The unexposed sister cell is out of view near the top of the image. Nucleoli can be seen to begin to form after about 30 min, as round domains that exclude chromatin and can be followed into G1.

Local fluorescence intensity reflects the concentration of histone H2B at that position and thus is a measure for the local state of compaction of chromatin. We have quantified how the intensity distribution, and therefore the compaction of chromatin, changes during transition from anaphase into G1. Figure 3A shows four mid-nuclear optical sections from the time series of 3D images shown in Figure 1, now color-coded for the local chromatin density (red: high density; blue: low density). The histograms in Figure 3B represent the fluorescence intensity distribution in four of the 3D images. The blue, green, orange and red curves represent the distributions at 0, 6, 21 and 140 min, respectively. All curves dispose a tail on the left side of the plot (at low intensities), which is mainly due to edge effects related to the limited

Figure 3. Quantitative analysis of chromatin decondensation. **(A)** In the selection of four mid-nuclear optical sections of a same time sequence (at 0, 6, 21 and 140 min), the false colors represent relative local chromatin density (red: highest density, purple: lowest density). After only 21 min, differences in chromatin density appear. **(B)** Fluorescence intensity histograms represent the intensity distributions in the respective four 3D images of **(A)**. The blue, green, orange and red curves represent the distributions at 0, 6, 21 and 140 min, respectively. These distributions show that chromatin decondenses on average by a factor of five (compare the red and the blue curve). **(C)** Thirteen local maxima (green spots) and nine local minima (red spots) of intensity were tracked during chromatin decondensation. **(D)** shows how the average intensity of these maxima (red line) and minima (green line) decrease during decondensation. In compact chromatin domains decondensation stops after 30 min. For local minima of intensity (less compact chromatin and nucleoli) decondensation continues for about 2 hours. **(E)** Concomitantly, the nuclear volume increased by a factor of five. **(F)** The total fluorescence signal in the 3D images did not change during the imaging process, showing that photobleaching is negligible.

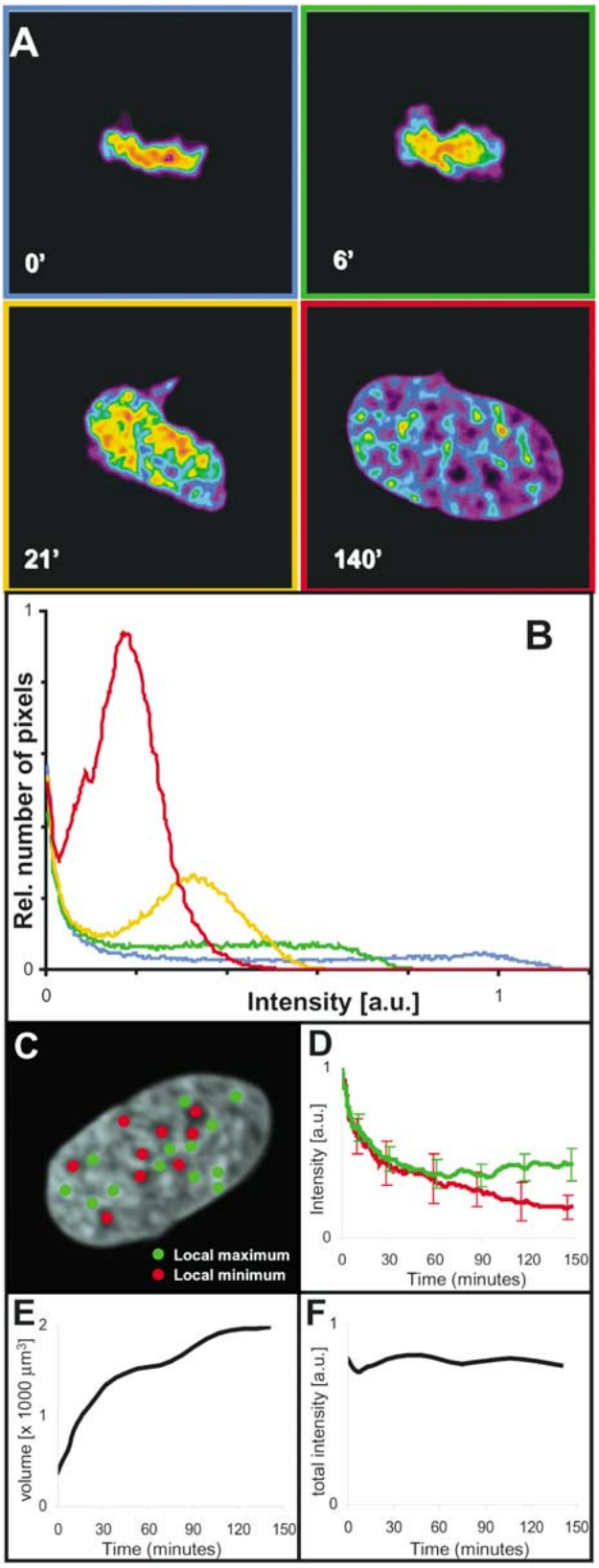
A
0'
6'
21'
140'
B
Rel. number of pixels
Intensity [a.u.]
C
Local maximum
Local minimum
D
Intensity [a.u.]
Time (minutes)
E
volume [x 1000 µm³]
Time (minutes)
F
total intensity [a.u.]
Time (minutes)

resolving power of the microscope. Results show that all chromatin decondenses upon entering G1. Intensities are scaled to the maximum of the blue curve ($t = 0$). The average degree of decondensation of the bulk of the chromatin is about a factor of five (compare the blue and the red histograms in Figure 3B).

Figure 3D shows the change in average intensity of thirteen compact chromatin domains (local maxima of intensity; green) and nine domains with low chromatin concentration (local minima of intensity, red), indicated as green and red dots in Figure 3C. Most of the decondensation takes place during the first 30 min after late anaphase, resulting in more than a two-fold decrease in average compaction. After that period, chromatin that remains relatively compact in interphase stops decondensing, reaching a final density of about 40–45% of the initial chromatin density (corresponding to the extreme right-hand tail of the histogram (red) in Figure 3B). Local minima of intensity continue to decondense down to about 20% of the initial chromatin density (corresponding with the extreme left tail of the histogram (red) in Figure 3B). Note that Figure 3D shows the progress of the average intensity of local minima and maxima. It shows that, during the first 30 min, the average intensities of final minima and maxima decrease at the same rate.

During decondensation, the nuclear volume increases by a factor of five to six, reaching its maximum volume after about 120 min (Figure 3E). The integrated nuclear fluorescence does not change during the imaging procedure, confirming that no photobleaching occurred during these experiments (Figure 3F).

Discussion

Large-scale chromatin organization is thought to be an important aspect of epigenetic regulation of gene expression. For instance, loci associated with heterochromatin domains in the nucleus are transcriptionally silent, whereas positioning of the loci away from heterochromatin permits transcription (Baxter *et al.* 2002). Genomic regulatory elements have been identified that control the local chromatin environment of genes (Francastel *et al.* 2000, Lundgren *et al.* 2000, Labrador & Corces 2002). The molecular mechanisms that underlie higher-order chromatin structure in nuclei are largely unknown. It is pertinent to ask how chromatin is positioned during assembly of the new interphase nucleus after mitosis. Here, we analyze this process by imaging the dynamic behavior of chromatin during the transition from late anaphase into G1. We have made and analyzed time series of confocal 3D images (4D imaging) of live HeLa cells that express GFP-tagged histone H2B (Kanda *et al.* 1998). These cells allow us to follow the dynamic behavior of chromatin as a new nucleus is assembled after cell division. The modified histone protein is evenly integrated into chromatin, like the endogenous histone H2B and the incorporation does not affect cell cycle behavior (Kanda *et al.* 1998). Experiments using FLIP (fluorescence loss in photobleaching) and FRAP (fluorescence recovery after photobleaching) techniques (Phair & Misteli 2000, Kimura & Cook 2001) have shown that essentially all histone H2B-GFP in the nucleus is bound and is incorporated into chromatin and that the exchange of bound histone H2B-GFP is slow. One therefore can use H2B-GFP as a marker that faithfully reflects chromatin concentration. Consequently, we have assumed the fluorescence signal from H2B-GFP to be proportional to local chromatin density.

A major problem in confocal 4D imaging of living cells is the phototoxicity of the light used for excitation of the fluorophore. In our experiments, the excitation light intensity was kept below 150 nW and the total exposure time of a cell that was 4D imaged for up to 3 h was not more than 70 s. Under these conditions, the total light dose was approximately $10\,\mathrm{J cm^{-2}}$ and no effect of excitation light on progression through mitosis was observed (Figure 1). At the same time, photobleaching was completely absent (Figure 3F), suggesting that bleaching and photodamage go hand-in-hand. If we used higher doses of light, we observed considerable phototoxic effects: i.e. cell cycle arrest. These findings agree well with studies on photochemotherapy, where fluorophores are used as photosensitizers (Bachor *et al.* 1991). They showed that phototoxic effects become evident at doses above about $10\,\mathrm{J\,cm^{-2}}$, depending on the fluorophore and the wavelength of the light. Importantly, our results demonstrate

that scanning confocal microscopy, using a standard confocal microscope, can be used to image processes in living cells in time and space at relatively high sampling rates (several 3D images per minute) over an extended period of time (several hours).

Our results show that the transition from late anaphase to G1 is accompanied by a predominantly radial expansion of chromatin (Figure 2). There is remarkably little relative movement of chromosomes and subchromosomal domains after late anaphase. Most chromatin domains that are neighbors in late anaphase are still adjacent in early G1. This result supports the observations of (Sullivan & Shelby 1999) that centromeres distribute into the newly formed nucleus by uniform isometric expansion of the bulk of the chromatin. Here we show that essentially all chromatin expands radially. These results show that there is only limited large-scale rearrangement of chromatin during the transition from anaphase to G1.

Recording of the spatial distribution of GFP-tagged chromatin as a function of time allowed us to analyze changes in local chromatin compaction. Four-dimensional image analysis shows that all chromatin decondenses by at least a factor of two (Figure 3D) and on average by a factor of five (Figure 3B). Clearly, no substantial chromatin domains remained as compact as in late anaphase, although we cannot exclude that chromatin domains that are much smaller than the point spread function of the microscope remain highly condensed. Evidently, the classical definition of heterochromatin, being 'the fraction of chromatin that does not decondense after mitosis' (Brown 1966), should be revised.

Our observations are compatible with the notion that, upon entering interphase, chromosomes decondense only to a limited extent, each occupying its own chromosome territory in the nucleus and not intermingling with other chromosomes (Cremer *et al.* 1993, Sadoni *et al.* 1999, Visser & Aten 1999, Visser *et al.* 2000). Our results on chromatin decondensation can now be compared with the reverse process, i.e. chromatin condensation during the G2–prophase transition (Manders *et al.* 1999). This process too involved remarkably limited overall movement of chromatin. The chromosomes just condensed at the position they occupied in late G2. It seems that, during mitosis in HeLa cells, a repositioning of chromosomes and large-scale reorganization of chromatin are very limited during both chromosome condensation and during chromosome decondensation. Chromosome positioning and large-scale chromatin structure may affect transcription and the timing of replication (Li *et al.* 2001; Heun *et al.* 2001; Gilbert 2002). Therefore, conservation of chromosome positioning and of large-scale chromatin structure throughout mitosis (from G2 to G1) is probably important for epigenetic gene control.

Evidence has been presented that transcriptionally active chromosomes are more likely to end up in the center of the nucleus, whereas less active ones tend to be more peripheral (Croft *et al.* 1999, Sadoni *et al.* 1999, Bridger *et al.* 2000, Boyle *et al.* 2001). Our results suggest that this aspect of nuclear organization is already implemented before late anaphase. Alternatively, rearrangements occur later in G1. In studies where relatively large chromosomes display a typical Rabl configuration immediately after mitosis, large-scale chromosomal movement has been observed during G1 (Csink & Henikoff 1998). Our analyses do not show such movements in HeLa cells, probably due to the absence of the Rabl configuration in interphase. Another constraint of chromosome positioning in the interphase nucleus is the formation of nucleoli, because different chromosomes contribute to these structures. The first indications of the assembly of nucleoli can already be seen as local chromatin-poor areas, as early as 20–30 min after anaphase (Figure 1). These observations agree with results of studies on the dynamic behavior of fibrillarin-GFP during the formation of nucleoli in telophase (Fomproix *et al.* 1998, Olson *et al.* 2000, Snaar *et al.* 2000).

Summarizing, our results show that, during the assembly of the new nucleus after mitosis, there is remarkably little relative movement of chromosomes and subchromosomal domains. If nuclear organization at this level is important for epigenetic control of gene expression, the correct relative arrangement of chromosomes and subchromosomal domains seems already to be established in late anaphase. Furthermore, our results indicate that essentially all chromatin decondenses after mitosis, albeit to a limited

extent. No chromatin remains as compact as in metaphase. Importantly, we show that good-quality 4D imaging of living cells with a relatively high rate is possible without detectable photo-damage, using a standard confocal microscopy.

Acknowledgements

The biological branch of the Netherlands Organization for Scientific Research financially supported this work (NWO-ALW grants: '4D-Imaging of Living Cells and Tissue' and 'Analyzing Biological Structures with Virtual Reality Techniques'). We thank Dr H. Kimura (University of Oxford, Oxford, UK) for kindly providing the HeLa histone H2B-GFP-expressing cell line.

References

Bachor R, Shea CR, Gillies R, Hasan T (1991) Photosensitized destruction of human bladder carcinoma cells treated with chlorin e6-conjugated microspheres. *Proc Natl Acad Sci USA* **88**: 1580–1584.

Baxter J, Merkenschlager M, Fisher AG (2002) Nuclear organisation and gene expression. *Curr Opin Cell Biol* **14**: 372–376.

Boyle S, Gilchrist S, Bridger JM, Mahy NL, Ellis JA, Bickmore WA (2001) The spatial organization of human chromosomes within the nuclei of normal and emerin-mutant cells. *Hum Mol Genet* **10**: 211–219.

Bridger JM, Boyle S, Kill IR, Bickmore WA (2000) Re-modelling of nuclear architecture in quiescent and senescent human fibroblasts. *Curr Biol* **10**: 149–152.

Brown SW (1966) Heterochromatin. *Science* **151**: 417–425.

Cmarko D, Verschure PJ, Martin TE *et al.* (1999) Ultrastructural analysis of transcription and splicing in the cell nucleus after bromo-UTP microinjection. *Mol Biol Cell* **10**: 211–223.

Cremer T, Kurz A, Zirbel R *et al.* (1993) Role of chromosome territories in the functional compartmentalization of the cell nucleus. *Cold Spring Harbor Symp Quant Biol* **58**: 777–792.

Croft JA, Bridger JM, Boyle S, Perry P, Teague P, Bickmore WA (1999) Differences in the localization and morphology of chromosomes in the human nucleus. *J Cell Biol* **145**: 1119–1131.

Csink AK, Henikoff S (1998) Large scale chromosomal movements during interphase progression in *Drosophila*. *J Cell Biol* **143**: 13–22.

De Leeuw WC, Van Liere R (2001) Chromatin decondensation: a case study of tracking features in confocal data. *IEEE Visualization* **2001**: 441–444.

De Leeuw WC, Van Liere R (2002) BM3D: motion estimation in time dependent volume data. *IEEE Visualization* **2002**: 427–434.

De Leeuw W, Van Liere R, Verschure P, Visser A, Manders E, Van Driel R (2000) Visualization of time dependent confocal microscopy data. *IEEE Visualization* **2000**: 473–476.

Fisher AG, Merkenschlager M (2002) Gene silencing, cell fate and nuclear organisation. *Curr Opin Genet Devel* **12**: 193–197.

Fomproix N, Gebrane Younes J, Hernandez Verdun D (1998) Effects of anti-fibrillarin antibodies on building of functional nucleoli at the end of mitosis. *J Cell Sci* **111**: 359–372.

Francastel C, Schubeler D, Martin DIK, Groudine M (2000) Nuclear compartmentalization and gene activity. *Nat Rev Mol Cell Biol* **1**: 137–143.

Gilbert DM (2002) Replication timing and transcription control: beyond cause and effect. *Curr Opin Cell Biol* **14**: 377–383.

Hens L, Bauman M, Cremer T, Sutter A, Cornelis JJ, Cremer C (1983) Immunocytochemical localization of chromatin regions UV-microirradiated in S-phase or anaphase. *Exp Cell Res* **149**: 257–269.

Heun P, Laroche T, Raghuraman MK, Gasser SM (2001) The positioning and dynamics of origins of replication in the budding yeast nucleus. *J Cell Biol* **152**: 385–400.

Li F, Chen J, Izumi M, Butler MC, Keezer SM, Gilbert DM (2001) The replication timing program of the Chinese hamster beta-globin locus is established coincident with its repositioning near peripheral heterochromatin in early G1 phase. *J Cell Biol* **154**: 283–292.

Kanda T, Sullivan KF, Wahl GM (1998) Histone-GFP fusion protein enables sensitive analysis of chromosome dynamics in living mammalian cells. *Curr Biol* **8**: 377–385.

Kimura H, Cook PR (2001) Kinetics of core histones in living human cells: Little exchange of H3 and H4 and some rapid exchange of H2B. *J Cell Biol* **153**: 1341–1353.

Labrador M, Corces VG (2002) Setting the boundaries of chromatin domains and nuclear organization. *Cell* **111**: 151–154.

Lundgren M, Chow CM, Sabbattini P, Georgiou A, Minaee S, Dillon N (2000) Transcription factor dosage affects changes in higher order chromatin structure associated with activation of a heterochromatic gene. *Cell* **103**: 733–743.

Manders EMM, Stap J, Strackee J, Van Driel R, Aten JA (1996) Dynamic behavior of DNA replication domains. *Exp Cell Res* **226**: 328–335.

Manders EMM, Kimura H, Cook PR (1999) Direct imaging of DNA in living cells reveals the dynamics of chromosome formation. *J Cell Biol* **144**: 813–821.

Olson MOJ, Dundr M, Szebeni A (2000) The nucleolus: an old factory with unexpected capabilities. *Trends Cell Biol* **10**: 189–196.

Phair RD, Misteli T (2000) High mobility of proteins in the mammalian cell nucleus. *Nature* **404**: 604–609.

Sadoni N, Langer S, Fauth C *et al.* (1999) Nuclear organization of mammalian genomes: polar chromosome territories build up functionally distinct higher order compartments. *J Cell Biol* **146**: 1211–1226.

Snaar S, Wiesmeijer K, Jochemsen AG, Tanke HJ, Dirks RW (2000) Mutational analysis of fibrillarin and its mobility in living human cells. *J Cell Biol* **151**: 653–662.

Sullivan KF, Shelby RD (1999) Using time-lapse confocal microscopy for analysis of centromere dynamics in human cells. *Meth Cell Biol* **58**: 183–202.

Van Balen R, Ten Kate T, Koelma D, Mosterd B, Smeulders AWM (1994) ScilImage: a multi-layered environment for use and development of image processing software. In: Crowley H.I.C.a.J.L, ed. *Experimental Environments for Computer Vision and Image Processing*. Singapore: World Scientific Press, pp 107–126.

Verschure PJ, van der Kraan I, Manders EM, van Driel R (1999) Spatial relationship between transcription sites and chromosome territories. *J Cell Biol* **147**: 13–24.

Visser AE, Aten JA (1999) Chromosomes as well as chromosomal subdomains constitute distinct units in interphase nuclei. *J Cell Sci* **112**: 3353–3360.